Direct Decomposition of NO on Ba Catalysts Supported on Ce–Fe Mixed Oxides

AUTHOR(S):

Hong, Won-Jong; Iwamoto, Shinji; Inoue, Masashi

CITATION:

Hong, Won-Jong ...[et al]. Direct Decomposition of NO on Ba Catalysts Supported on Ce–Fe Mixed Oxides. Catalysis Letters 2010, 135(3-4): 190-196

ISSUE DATE:

2010-04

URL:

http://hdl.handle.net/2433/128948

Direct decomposition of NO on Ba catalysts supported on Ce–Fe mixed oxides

Won-Jong Hong[1], Shinji Iwamoto[2], Masashi Inoue[1*]

[1]Department of Energy and Hydrocarbon Chemistry
Graduate School of Engineering, Kyoto University, Kyoto, 615-8510, JAPAN

[2]Department of Chemistry and Chemical Biology,
Graduate School of Engineering, Gunma University, Tenjin, Kiryu 376-8515, JAPAN

[*] Corresponding author

Tel.: +81-75-383-2478

Fax: +81-75-383-2479

E-mail address: inoue@scl.kyoto-u.ac.jp

Abstract

Cerium-iron mixed oxides were prepared by a glycothermal method, and NO decomposition reactions over these oxides and barium catalysts supported on them were examined. Although Ce–Fe mixed oxides (Ce–Fe(x), x = Fe/(Ce+Fe) molar ratio) exhibited only low activities for the direct decomposition of NO into N_2 and O_2, Ba catalysts supported on these mixed oxides are active for this reaction. The highest NO conversion was achieved with 3 wt% BaO/Ce–Fe(0.02). The NO conversion on this catalyst increased with increasing reaction temperature, and NO conversion was 51 % at 800 °C. The high activity of this catalyst was maintained for more than 10 h and a relatively high NO conversion (23 %) was obtained even in the presence of 5 % oxygen. The XRD results indicated the formation of Ce–Fe(x) solid solutions with a cubic fluorite structure. The CO_2-TPD results indicated NO decomposition activities of the catalysts were correlated with their basicities.

1. Introduction

Exhaust gases from vehicle engines and industrial combustion facilities contain considerable amounts of nitrogen oxides (NO_x), which cause severe environmental problems. Practical NO_x emission control technologies such as three-way catalyst method for gasoline-fueled vehicles, NO_x storage-reduction (NSR) catalysts for lean-burn engine systems, and SCR processes for large-scale boilers have been developed; however, there is still a great research interest for the development of novel and more efficient deNO_x methods. Among various deNO_x strategies, direct decomposition of NO ($NO \rightarrow 1/2O_2 + 1/2N_2$) has been considered to be the most desirable method because this reaction is thermodynamically favorable at low temperatures and does not need any reductants such as NH_3, H_2, CO, or hydrocarbons. Hence, this reaction receives special interest of scientists, although no practical application has been reported until now.

A number of catalysts have been examined for this reaction, and several types of catalysts, such as precious metals [1,2], ion-exchanged zeolites [3,4], single-component metal oxides [5,6], and perovskites [7–10], were found to be active for this reaction. Recently, Imanaka et al. examined the direct NO decomposition on Gd–Y–Ba oxides [11] and Y–Zr oxides [12] with C-type cubic crystal structure and reported that these catalysts exhibited higher activities than the conventional perovskite-type catalysts. However, N_2 selectivity was quite low at temperatures below 600 °C. Accordingly, it is necessary to develop new active catalysts which can show both low-temperature activity and high thermal-stability.

We found that Ba–Ce–Co mixed oxides, composed of three phases, CeO_2, Co_3O_4, and $BaCeO_{3-\delta}$, showed high activities for NO decomposition reaction [13]. Then, to examine

the active sites of the catalysts, Ba catalysts supported on Co_3O_4 and CeO_2 were prepared, and it was found that the reaction rate was correlated to the number of basic sites of the catalysts [14].

Because of their unique oxygen-storage and redox properties, Ce-based mixed oxides have been widely used in many catalyses, such as catalytic conversion of light hydrocarbons [15], liquid phase oxidation reaction [16], and treatment of exhaust gases [17]. Therefore, the addition of the second component to CeO_2 was examined and it was found that Ba catalysts supported on Ce–Mn mixed oxides showed significantly improved activities for direct decomposition of NO [18]. In a previous paper [18], we also found that the addition of Fe to CeO_2 with Fe/Ce of 0.1 was also effective to improve the activity, although the promotion effect of Fe for CeO_2 was less significant as compared to that of Mn. However, iron is less expensive and environmentally harmless, which motivated us to explore the Ce–Fe system further. In this study, we prepared Ce–Fe mixed oxides with various Ce/Fe ratios, and the NO decomposition activities of Ce–Fe oxide catalysts and Ba catalysts supported on them were examined. The catalysts were characterized by several techniques and correlation between NO decomposition activities and physicochemical properties of the catalysts was investigated.

2. Experimental

2.1. Preparation of the catalysts

Ce–Fe oxide samples (designated as Ce–Fe(x), x = Fe/(Ce+Fe) molar raio) were prepared by a glycothermal method. Appropriate amounts of $Ce(CH_3COO)_3{\cdot}4H_2O$ and $Fe(CH_3COO)_2$ were added to 100 ml of 1,4-butanediol, and this mixture was set in a

300-ml autoclave. After the atmosphere inside the autoclave was completely replaced with nitrogen, the autoclave was heated to 300 °C at a rate of 2.3 °C min^{-1} and kept at that temperature for 2 h. After cooling, the resultant powder product was collected by centrifugation, washed with acetone, air-dried, and calcined at 400 °C in air for 4 h.

Barium (up to 10 wt% as BaO) was loaded on Ce–Fe(*x*) by an impregnation method using an aqueous solution of barium nitrate, and the precursor was calcined at 800 °C for 1 h (designated as BaO/Ce–Fe(*x*)).

2.2. Direct NO decomposition reaction

The NO decomposition reaction was carried out in a fixed-bed flow reactor made of quartz glass tubing with an inner diameter of 10 mm. The catalysts were pressed into a pellet, pulverized into 10 to 22 mesh size, and charged to the reactor. After the catalyst bed was heated to 800 °C in a He flow, the reaction gas composed of 6000 ppm NO and 0–5% O_2 (He balance) was fed over 0.50–1.0 g of the catalysts at a rate of 20–300 ml min^{-1} (W/F = 0.2–3 g s ml^{-1}). The effluent gas was analyzed using a GL Science MicroGC 2002 gas chromatograph equipped with Molsieve 5A and Poraplot Q columns. The NO conversion was expressed on the basis of the formation of N_2:

$$\text{NO conversion} = \frac{2[N_2]_{out}}{[NO]_{in}},$$

where $[NO]_{in}$ and $[N_2]_{out}$ are concentrations of NO in the feed and of N_2 in the effluent, respectively.

Only a small amount of the by-product, N_2O, was formed for all the catalysts tested.

2.3. Characterization of the catalysts

Powder X-ray diffraction (XRD) patterns were recorded on a Rigaku RINT 2500 X-ray diffractometer using CuKα radiation (scan rate, 0.02 ° 2θ min^{-1}). Crystallite sizes of CeO_2 were calculated from the half-height width of the 111 diffraction peak (2θ = 28.55 °) using the Scherrer equation. Specific surface areas were calculated by the BET single-point method on the basis of nitrogen uptakes measured at 77 K using a Micromeritics Flowsorb II 2300 sorptograph. The samples were evacuated at 300 °C for 30 min prior to the measurement.

Temperature-programmed desorption of CO_2 (CO_2-TPD) was carried out on a Bel Japan TPD-1-AT apparatus with a Q-MASS detector. Before performing CO_2-TPD experiment, the sample (50 mg) was treated in situ in a 50 ml min^{-1} 20% O_2–He flow at 800 °C for 1 h, cooled to 50 °C in the same atmosphere, and purged with a 50 ml min^{-1} He flow for 30 min. The sample was exposed to a 20 ml min^{-1} flow of 19% CO_2 for 30 min, purged again with a 50 ml min^{-1} He flow for 30 min, and then heated in the same flow from 50 °C to 800 °C at a rate of 10 °C min^{-1} with monitoring the CO_2 desorption.

3. Results and Discussion

3.1. NO decomposition on Ba catalysts supported on Ce–Fe mixed oxides

Figure 1 shows the NO decomposition activities of Ce–Fe(x) and 7 wt% BaO/Ce–Fe(x) with various Fe contents. The Ce–Fe(x) mixed oxides showed quite low activities irrespective of the Fe contents. On the contrary, the Ba-loaded catalysts showed significant activities. As compared with the Ba catalysts supported on single-component carriers, CeO_2 (x = 0) and Fe_2O_3 (x = 1), which exhibited 18% and 5% of NO conversions, respectively, the Ba catalysts supported on Ce–Fe mixed oxides

showed enhanced activities. The highest activity was observed for 7 wt% BaO/Ce–Fe(0.02); 46% NO conversion to N_2 was attained at 800 °C.

Figure 2 shows the effect of the amount of BaO on the activity of the BaO/Ce–Fe(0.02) catalysts. Without the addition of BaO, the NO conversion was very low; however, the BaO loading significantly increased the activity, suggesting that Ba species is related to the active sites. The highest NO conversion was attained with 3 wt% BaO/Ce–Fe(0.02), and further increase in the BaO loading caused a gradual decrease in the activity. In the XRD pattern of the catalyst with 10 wt% BaO, small diffraction peaks due to $BaCO_3$ were detected, indicating low dispersion of the Ba species in this catalyst.

Figure 3 shows the stability of 3 wt% BaO/Ce–Fe(0.02) for the NO decomposition. At 550 ºC, the conversion of NO to N_2 at the initial stage was 3% and it did not decrease after 10 h on stream, indicating that oxygen atoms formed by decomposition of NO were not accumulated on the catalyst. At 800 ºC, a stable NO conversion, as high as 60%, was preserved over 10 h.

Figure 4 shows the effect of W/F on the NO decomposition on the 3 wt% BaO/Ce–Fe(0.02) catalyst measured by changing the flow rate. The NO conversion gradually increased with increasing the contact time. At 800 ºC, quite a high NO conversion (75%) was attained at W/F = 3.0 g s ml^{-1}. On the other hand, even at a short contact time of W/F = 0.2 g s ml^{-1}, the catalyst exhibited 35% of NO conversion, indicating the high performance of this catalyst.

3.2. Characterization of the Ba catalysts supported on Ce–Fe mixed oxides

Figure 5 presents the XRD patterns of the 7 wt% BaO/Ce–Fe(x) catalysts. Diffraction peaks due to the CeO_2 phase with a cubic fluorite structure was recognized for all the catalysts except BaO/Ce–Fe(1). For $x \geq 0.5$, diffraction peaks due to Fe_2O_3 (JCPDS #39-1346) were observed in addition to the CeO_2 peaks. However, for $x \leq 0.17$, only diffraction peaks due to CeO_2 were observed, and no diffraction peaks due to Fe- and Ba-containing phases were recognized, indicating that Fe and Ba ions were highly dispersed in these catalysts.

Figure 6 shows the lattice parameters of the CeO_2 phase for Ce–Fe(x) calcined at 400 ºC and for BaO/Ce–Fe(x) calcined at 800 ºC. For the Ce–Fe(x) samples without BaO, the lattice parameter decreased remarkably with increasing Fe content, indicating the dissolution of Fe ions into the CeO_2 structure. However, the lattice parameter for $x = 0.5$ was almost same as that for $x = 0.17$, suggesting the existence of limitation of the Fe incorporation. This result is consistent with the report by Li et al. [19], who found that the $Ce_{1-x}Fe_xO_2$ solid solutions can be synthesized by a hydrothermal method until $x = 0.15$. For BaO/Ce–Fe(0), the lattice parameter was larger than that of CeO_2, indicating the incorporation of Ba ions into the fluorite structure. In the BaO–CeO_2 system, only one binary compound $BaCeO_3$ is found [20], and it is generally believed that Ba^{2+} ion does not dissolve in the CeO_2 matrix because ionic radius of Ba^{2+} is much larger than that of Ce^{4+} [21]. However, these statements do not rule out the possibility for the formation of the BaO–CeO_2 solid solution as a metastable phase. Actually, Ba-doped CeO_2 samples have been prepared and a large expansion of the lattice parameter of CeO_2 has been reported [22,23]. Pt–Ba–CeO_2 catalysts have been widely examined for the NO_x–storage–reduction strategy [24–30]. Although the phases developed by thermal treatment of these catalysts have been carefully examined, BaO–CeO_2 solid solutions

have never been detected in these works [24–26,31]. This is presumably because the catalysts were prepared by impregnation of CeO_2 with a barium acetate solution. Thermal decomposition of the acetate gives barium carbonate which is loaded on outer surface of ceria particles. Barium carbonate is fairly stable and the decomposition of this phase causes the formation of $BaCeO_3$. In the present work, the CeO_2 sample prepared by the glycothermal method was impregnated with an aqueous solution of barium nitrate. Since the glycothermally prepared crystals have various types of defects [32,33], Ba^{2+} ions seems to be able to migrate into the CeO_2 matrix. For comparison, a 7wt% BaO/Ce–Fe(0.02) catalyst was prepared by impregnation of Ce–Fe(0.02) with an aqueous solution of barium acetate. As expected this catalyst showed a lower activity for direct decomposition of NO (data not shown) than the catalyst prepared from barium nitrate.

For the BaO/Ce–Fe(x) samples, the lattice parameter increased with the increase in x up to 0.05, suggesting that a larger amount of Ba was soluble in the $Ce_{1-x}Fe_xO_2$ solid solution. However, further increase in x caused a gradual decrease in the lattice parameters of the CeO_2 phase.

In Table 1, physical properties of Ce–Fe(x) and BaO/Ce–Fe(x) are summarized. The addition of a small amount of Fe to CeO_2 increased the BET surface area of the product. However, the BET surface areas of Ce–Fe(x) drastically decreased by calcination at 800 °C. For Ce–Fe(x) with $x \geq 0.09$, the surface area gradually decreased with increasing the Fe content. This tendency was also observed for BaO/Ce–Fe(x), and the crystallite size as well decreased with increasing the Fe content. When each primary particle is a single crystal, BET surface area should increase with the decrease in the crystallite size. Therefore, the primary particles of the present products are composed of

mosaic of crystallites. The correlation between the BET surface area and catalytic activities was not observed.

In order to estimate the basicity of the catalysts, CO_2-TPD experiments were carried out and the results are shown in Figure 7. The desorption profile for single-component CeO_2 showed a peak around 100 °C. On the contrary, the BaO-loaded CeO_2 samples showed a very broad peak at temperatures higher than 100 °C, indicating that they have considerably strong basic sites on the surface. Interestingly, the CO_2 uptake for BaO/Ce–Fe(0.02) was much larger than that of BaO/Ce–Fe(0), indicating an increase in the number of basic sites. In Figure 8, effect of x on the CO_2 uptake of the BaO/Ce–Fe(x) catalysts is shown. Although pure CeO_2 showed a significant CO_2 uptake, the BaO loading apparently increased the CO_2 uptake. Furthermore, the addition of Fe increased the CO_2 uptake markedly. This feature is probably due to the oxygen defects caused by the dissolution of Fe ions into the CeO_2 structure. The maximum CO_2 uptake was attained for the samples with x = 0.02, and further increase in the Fe content gradually decreased CO_2 uptake. This tendency is similar to the effect of Fe on the NO decomposition activity as shown in Figure 1, indicating that the NO decomposition activity of the catalyst is controlled by its basic property. As shown in Figure 6, a similar behavior was also observed in the change in the unit cell parameter of the CeO_2 phase, which suggests that the Ba species highly dispersed in the fluorite structure is the origin of the basic sites of the catalysts.

3.3. Influence of O_2 on the NO decomposition activity of BaO/Ce–Fe(0.02) catalyst.

The effect of the addition of oxygen to the reaction gas was investigated using 3 wt% BaO/Ce–Fe(0.02), since it is well known that oxygen suppresses the activities of NO

decomposition catalysts [8, 34]. Figure 9 shows NO conversion at 800 ºC as a function of O_2 concentration. The NO conversion monotonically decreased with increasing the O_2 concentration. However, even in the presence of 5% O_2, the 3 wt% BaO/Ce–Fe(0.02) catalyst preserved a relatively high activity, 23%, at 800 ºC. The reaction order with respect to the O_2 partial pressure became negatively large with decreasing the reaction temperature, indicating that retarding effect of oxygen become more significant at lower temperatures. However, the reaction order with respect to the O_2 partial pressure at 800 ºC was -0.29 (Figure 10). The absolute value of this reaction order was relatively small, suggesting a potential of the present catalyst for practical deNOx applications.

4. Conclusions

The direct decomposition of NO over Ba catalysts supported on Ce–Fe mixed oxides was examined, and it was found that Ba catalysts supported on Ce–Fe(0.02) mixed oxides exhibited quite high activities. The XRD analyses indicated that the Ce–Fe solid solutions with a cubic fluorite structure were formed. The CO_2-TPD results indicated the NO decomposition activities of the catalysts correlated with their basic properties. A high NO conversion, 60% at 800 ºC in the absence of O_2 was attained over 3 wt% BaO/Ce–Fe(0.02), and even in the presence of 5% oxygen, this catalyst showed 23% NO conversion. The catalyst maintained the activity for over 10 h, suggesting a high potential of BaO/Ce–Fe mixed oxide catalysts for practical application in NOx emission control.

Acknowledgments

This work was supported by a Grant-in-Aid from Ministry of Education, Culture, Sports, Science and Technology, Japan.

5. References

1. A. Amernazmi, J. E. Benson, M. Boudart, J. Catal., 30 (1973) 55.

2. R. J. Wu, T. Y. Chou, C. T. Yeh, Appl. Catal. B: Environ., 6 (1995) 105.

3. M. Iwamoto, H. Yahiro, Y. Mine, S. Kagawa, Chem. Lett., 18 (1989) 213.

4. M. Iwamoto, H. Hamada, Catal. Today, 10 (1991) 57.

5. E. R. S. Winter, J. Catal., 22 (1971) 158.

6. E. R. S. Winter, J. Catal., 34 (1974) 440.

7. Y. Teraoka, H. Fukuda, S. Kagawa, Chem. Lett., 19 (1990) 1.

8. Y. Teraoka, T. Harada, S. Kagawa, J. Chem. Soc. Faraday Trans., 94 (1998) 1887.

9. H. Iwakuni, Y. Shinmyou, H. Yano, H. Matsumoto, T. Ishihara, Appl. Catal. B: Environ., 74 (2007) 299.

10. H. Iwakuni, Y. Shinmyou, H. Matsumoto, T. Ishihara, Bull. Chem. Soc. Jpn., 80 (2007) 2039.

11. N. Imanaka, T. Masui, H. Masaki, Adv. Mater., 19 (2007) 3660.

12. H. Masaki, T. Masui, N. Imanaka, J. Alloys Compd., 451 (2008) 406.

13. S. Iwamoto, T. Yasuda, M. Inoue, Adv. Tech. Mater. Mater. Proc. J., 4 (2002) 58.

14. S. Iwamoto, T. Yasuda, Y. Kouno, M. Inoue, Adv. Sci. Tech., 33 (2003) 375.

15. C. Padeste, N. W. Cant, D. L. Trimm, Catal. Lett., 18 (1993) 305.

16. H. C. Shen, H. S. Weng, Ind. Eng, Chem. Res., 29 (1990) 713.

17. P. Fornasiero, R. Di Monte, G. Ranga Rao, J. Kapar, S. Meriani, A. Trovarelli, M. Graziani, J. Catal., 151 (1995) 168.

18. S. Iwamoto, R. Takahashi, M. Inoue, Appl. Catal. B: Environ., 70 (2007) 146.

19. G. Li, R. L. Smith, H. Inomata, J. Am. Chem. Soc., 123 (2001) 11091.

20. J. P. Guha, D. Kolar, J. Mater. Sci., 6 (1971) 1174.

21. J. G. Nunan, M. J. Cohn, J. T. Donner, Catal. Today, 14 (1992) 277.

22. M. Radović, Z. Dohčević-Mitrović, M. Šćepanović, M. Grujić-Brojčin, B. Matović, S. Bošković, Z. V. Popović, Sci. Sinter., 39 (2007) 281.

23. Z. Zhang, C. Hu, Y. Xiong, R. Yang, Z. L. Wang, Nanotechnology, 18 (2007) 465504 (5pp).

24. M. Eberhardt, R. Riedel, U. Gőbel, J. Theis, E. S. Lox, Top. Catal., 30/1 (2004) 135.

25. M. Piacentini, M. Maciejewski, A. Baiker, Appl. Catal. B: Environ., 66 (2006) 126.

26. M. Casapu, J.-D. Grunwaldt, M. Maciejewski, M. Wittrock, U. Göbel, A. Baiker, Appl. Catal. B: Environ., 63 (2006) 232.

27. R. Strobel, F. Krumeich, S. E. Pratsinis, A. Baiker, J. Catal., 243 (2006) 229.

28. M. Piacentini, M. Maciejewski, A. Baiker, Appl. Catal. B: Environ., 72 (2007) 105.

29. M. Casapu, J.-D. Grunwaldt, M. Maciejewski, Alfons Baiker, S. Eckhoff, U. Göbel, M. Wittrock, J. Catal., 251 (2007) 28.

30. M. Casapu, J.-D. Grunwaldt, M. Maciejewski, F. Krumeich, A. Baiker, M. Wittrock, S. Eckhoff, Appl. Catal. B: Environ., 78 (2008) 288.

31. M. A. Peralta, V. G. Milt, L. M. Cornaglia, C. A. Querini, J. Catal., 242 (2006) 118.

32. M. Inoue, Adv. Sci. Technol., 29 (2000) 855.

33. S. Hosokawa, Y. Tanaka, S. Iwamoto, M. Inoue, J. Alloys Compd., 451 (2008) 309.

34. T. Ishihara, M. Ando, K. Sada, K. Takiishi, K. Yamada, H. Nishiguchi, Y. Takita, J. Catal., 220 (2003) 104.

Table 1. Physical properties of Ce–Fe(*x*) and 7 wt% BaO/Ce–Fe(*x*) catalysts.

x	BET surface area ($m^2\ g^{-1}$)			Crystallite size[a)] (nm)		
	A	B	C	A	B	C
0	132	36	24	8	25	29
0.01	138	30	12	8	28	23
0.02	147	29	12	9	24	23
0.032	150	32	16	11	23	23
0.048	151	23	13	N.D.	N.D.	21
0.09	153	23	19	N.D.	N.D.	18
0.17	146	19	17	N.D.	N.D.	16
0.5	106	18	17	6	21	15
0.75	83	12	14	8	20	14
1	22	3	5	–	–	–

a) Calculated from the 111 diffraction peak of the fluorite phase.
A : Ce-Fe(*x*) calcined at 400 ºC for 4 h.
B : Ce-Fe(*x*) calcined at 800 ºC for 1 h.
C : 7wt% BaO/Ce-Fe(*x*) calcined at 800 ºC for 1 h.

Figure captions

Figure 1. NO conversion to N_2 on Ce–Fe(*x*) and 7 wt% BaO/Ce–Fe(*x*) as a function of *x*, Fe/(Ce+Fe) ratio in Ce–Fe oxide. Catalyst, 0.50 g; reaction gas, 6000 ppm NO in He; flow rate, 30 ml min^{-1} (W/F = 1.0 g s ml^{-1}); reaction temperature, 800 °C.

Figure 2. Effect of Ba loading on the NO decomposition activities of BaO/Ce–Fe(0.02) catalyst. Catalyst, 0.50 g; reaction gas, 6000 ppm NO in He; flow rate, 30 ml min^{-1} (W/F = 1.0 g s ml^{-1}).

Figure 3. Duration test of 3 wt% BaO/Ce–Fe(0.02) catalysts for direct decomposition of NO. Catalyst, 1.0 g; reaction gas, 6000 ppm NO in He; flow rate, 60 ml min^{-1} (W/F = 1.0 g s ml^{-1}).

Figure 4. NO decomposition on 3 wt% BaO/Ce–Fe(0.02) catalyst as a function of W/F. Catalyst, 1.0 g; reaction gas, 6000 ppm NO in He; flow rate, 20–300 ml min^{-1}.

Figure 5. XRD patterns of 7 wt% BaO/Ce–Fe(*x*) calcined at 800 °C.

Figure 6. Lattice parameters of CeO_2 for Ce–Fe(*x*) calcined at 400 °C and 7 wt% BaO/Ce–Fe(*x*) catalysts.

Figure 7. CO_2-TPD profiles of CeO_2 and 7 wt% BaO/Ce–Fe(x) calcined at 800 °C. Prior to the measurement, the sample was treated again in situ in a 20% O_2–He flow at 800 for 1 h.

Figure 8. Amount of CO_2 desorbed from CeO_2 and 7 wt% BaO/Ce–Fe(x) calcined at 800 °C.

Figure 9. Effect of oxygen on the NO decomposition activity of 3 wt% BaO/Ce–Fe(0.02) catalyst. Catalyst, 1.0 g; reaction gas, 4000 ppm NO and 0–5% O_2 in He; flow rate, 60 ml min^{-1} (W/F = 1.0 g s ml^{-1}).

Figure 10. N_2 formation rate on 3 wt% BaO/Ce–Fe(0.02) catalyst as a function of oxygen partial pressure.

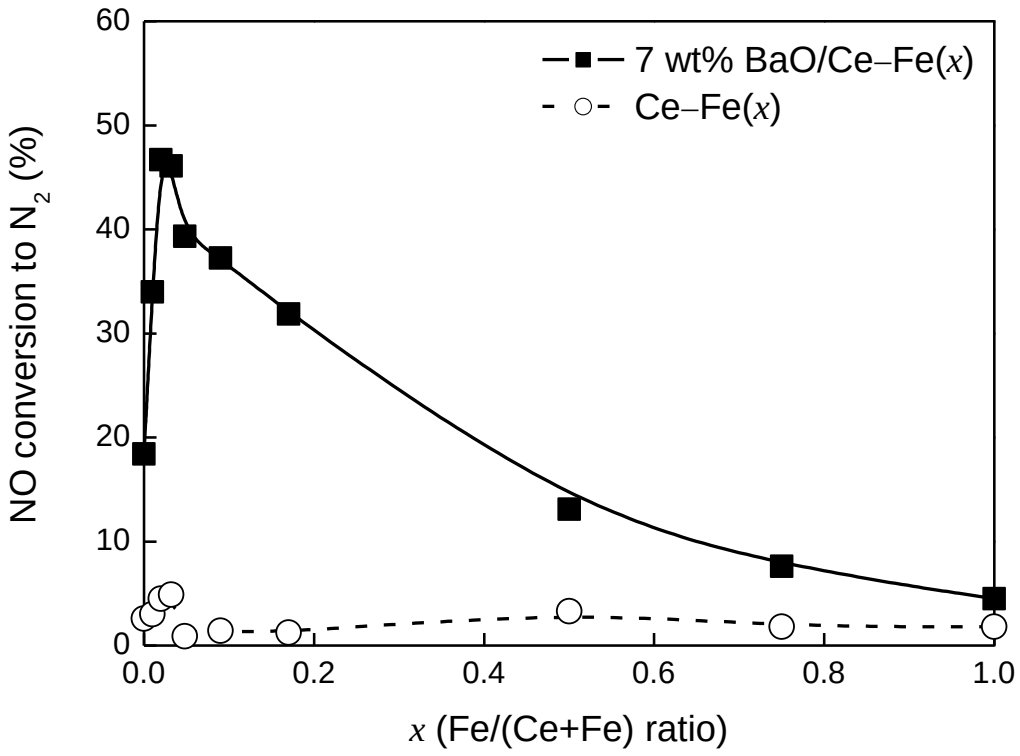

Figure 1. W.-J. Hong et al.

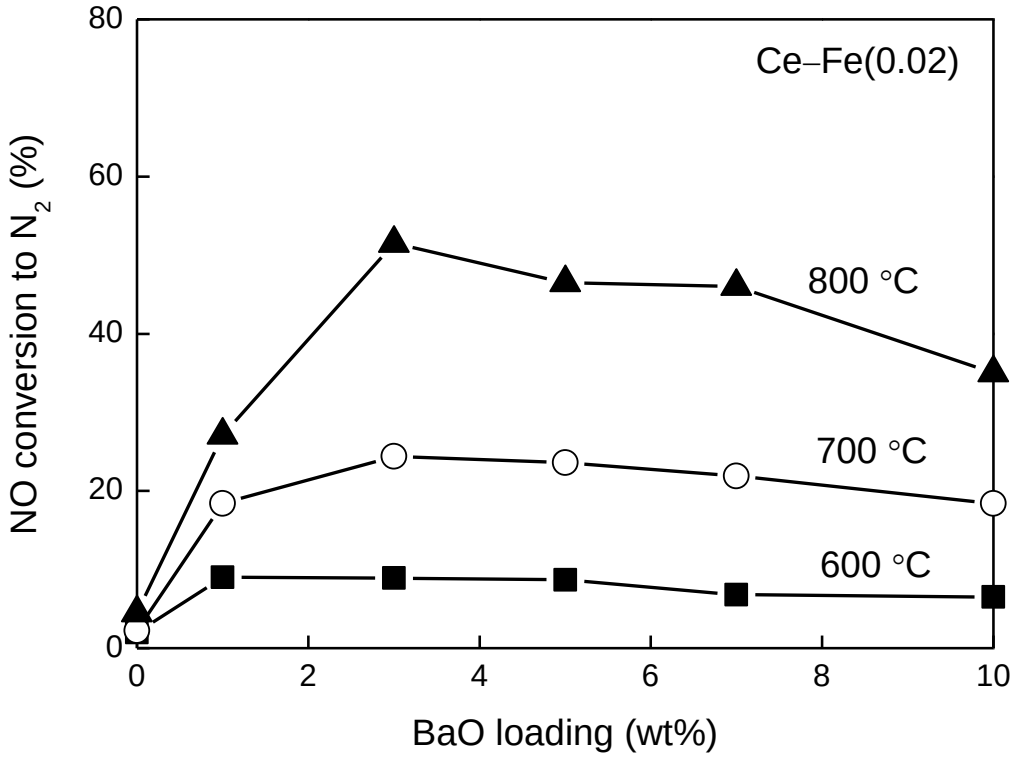

Figure 2. W.-J. Hong et al.

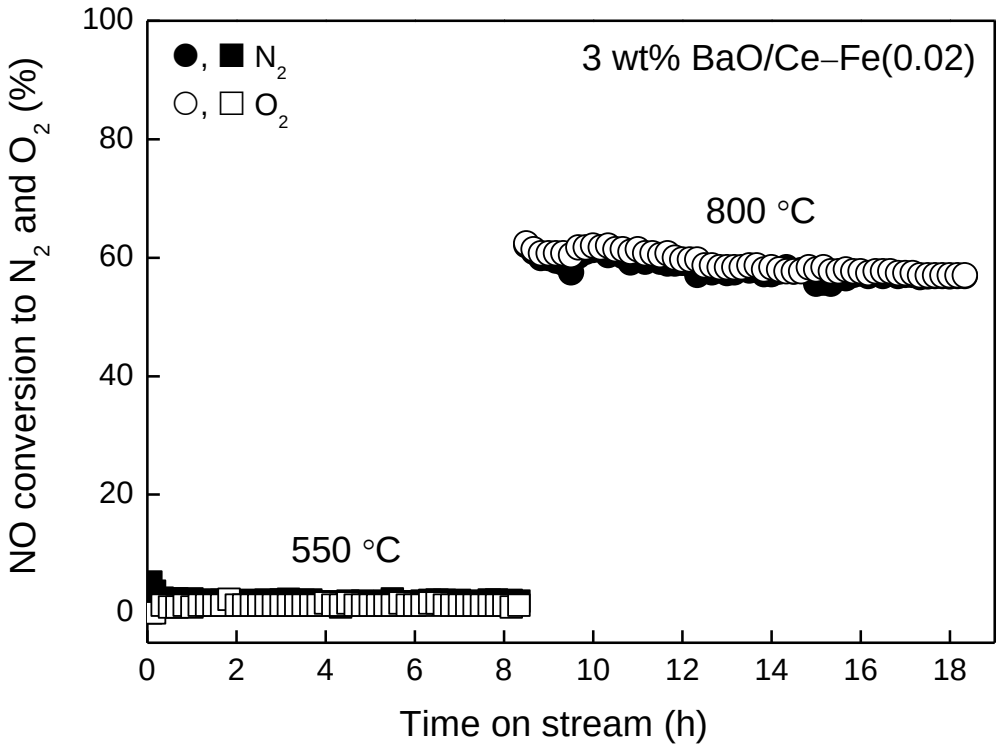

Figure 3. W.-J. Hong et al.

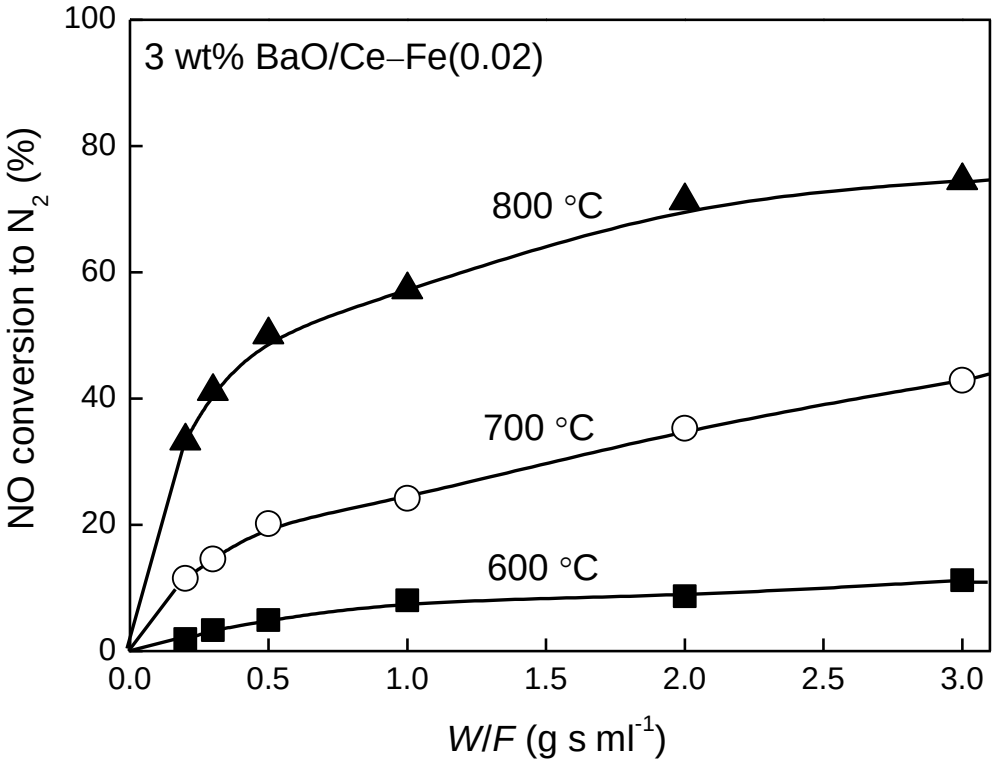

Figure 4. W.-J. Hong et al.

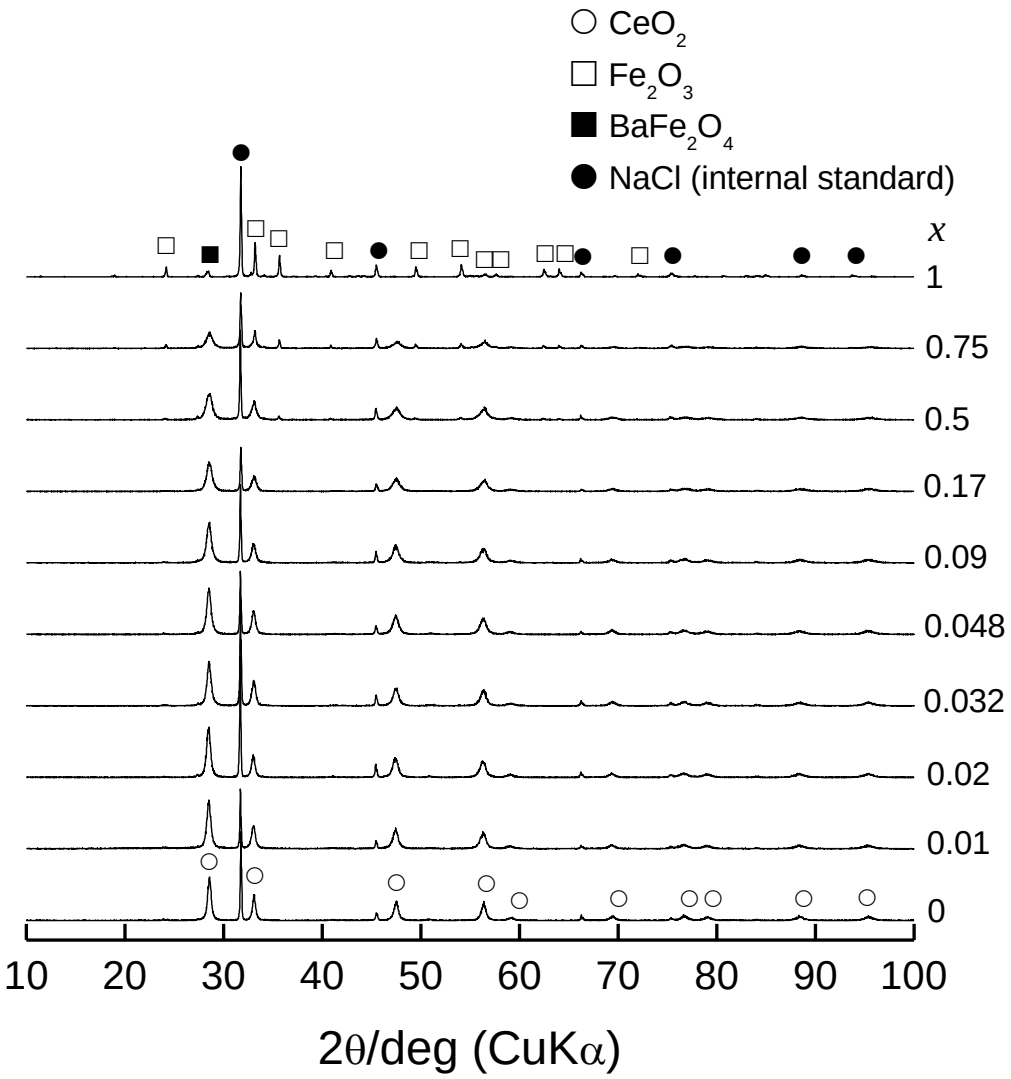

Figure 5. W.-J. Hong et al.

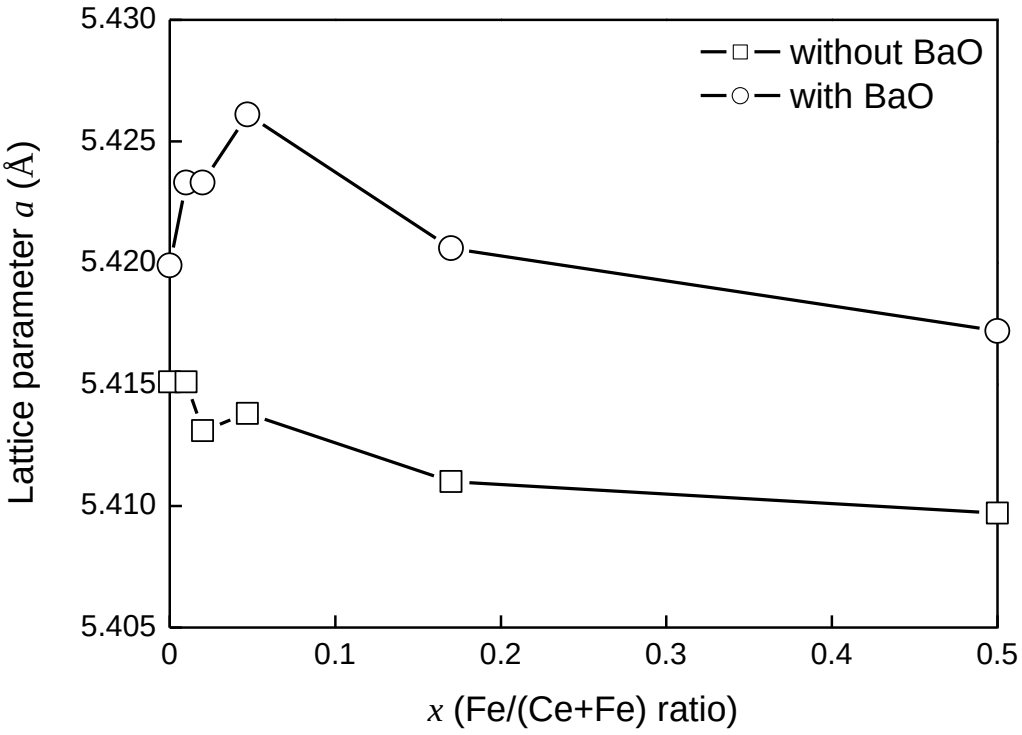

Figure 6. W.-J. Hong et al.

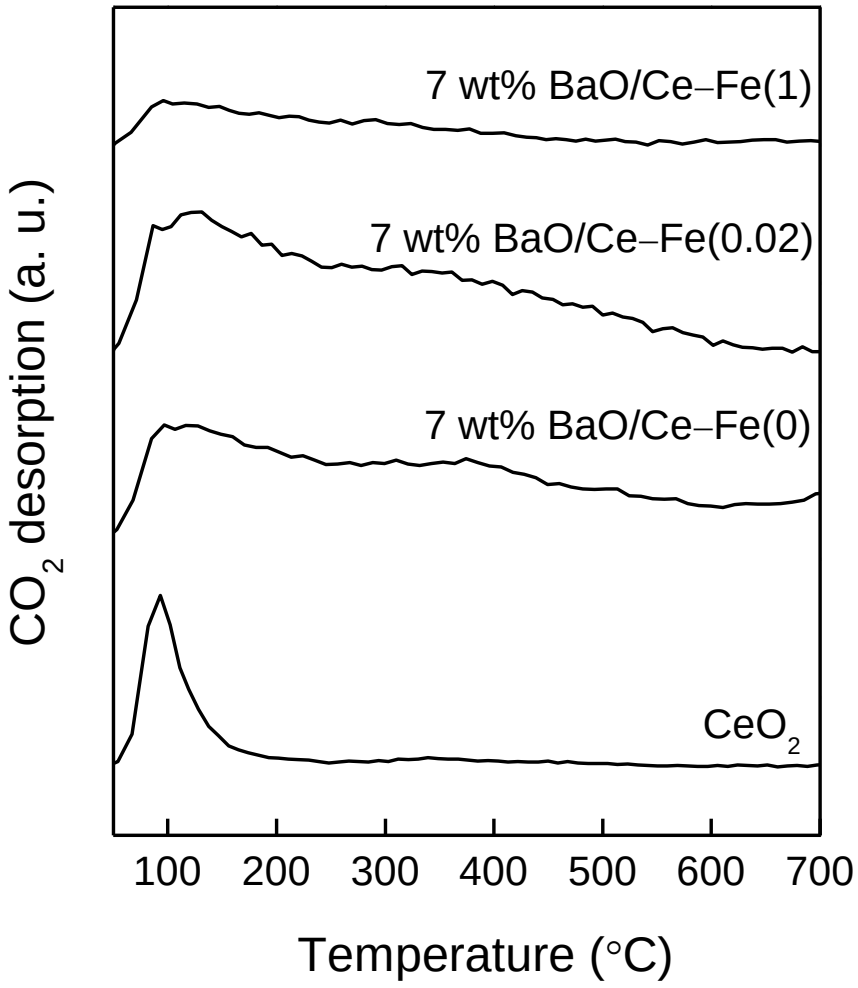

Figure 7. W.-J. Hong et al.

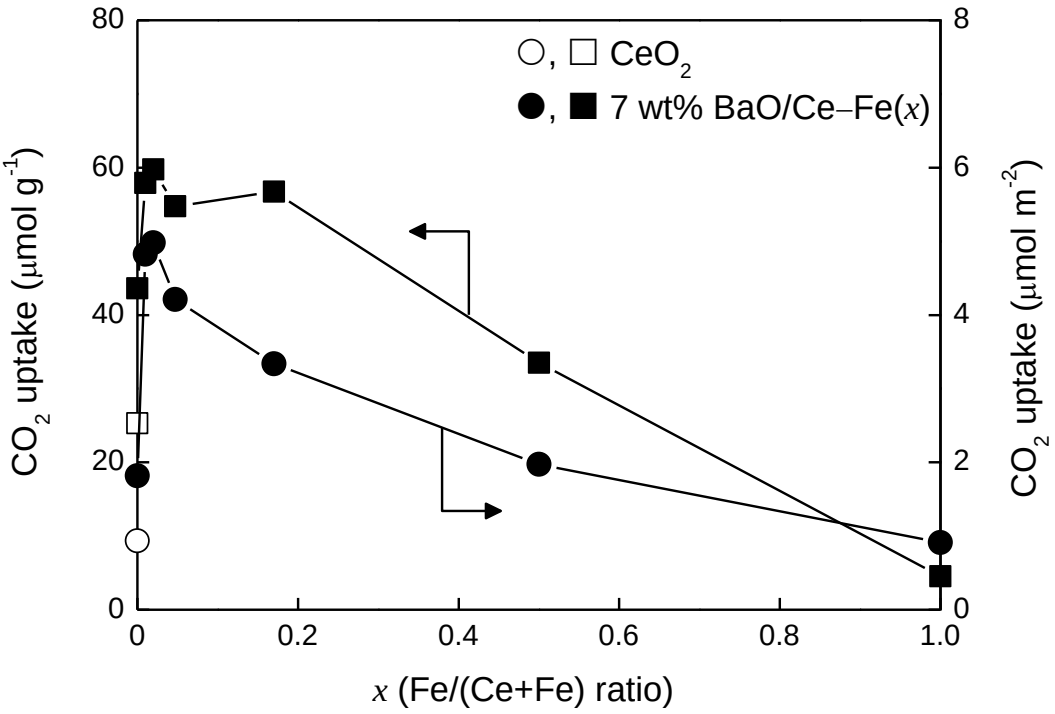

Figure 8. W.-J. Hong et al.

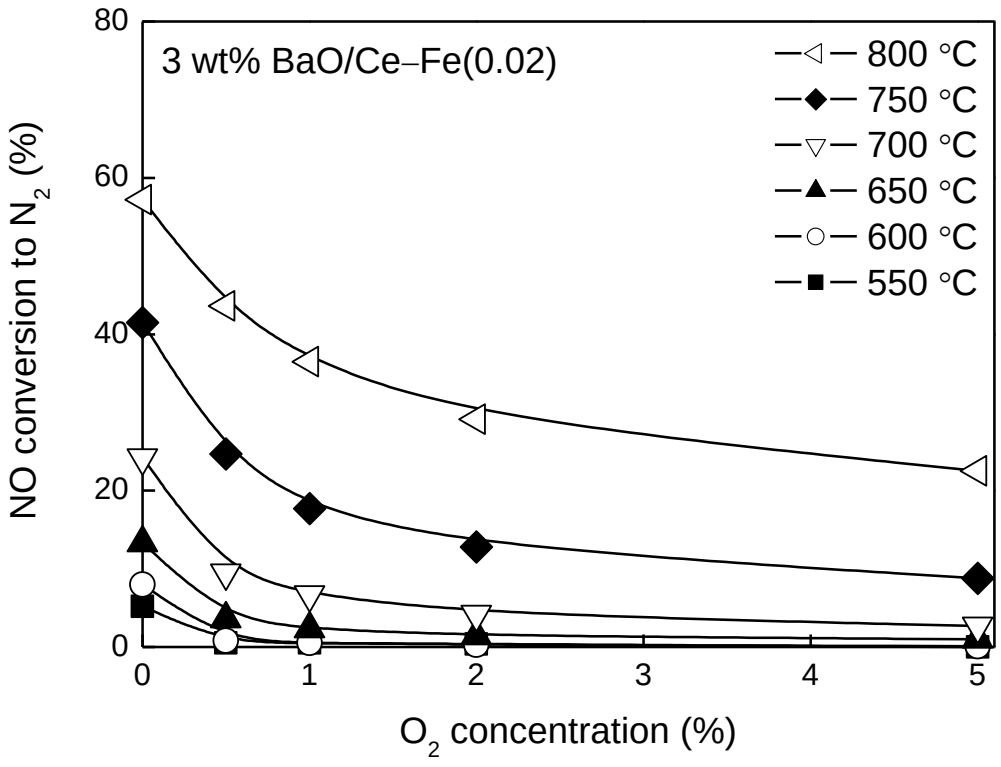

Figure 9. W.-J. Hong et al.

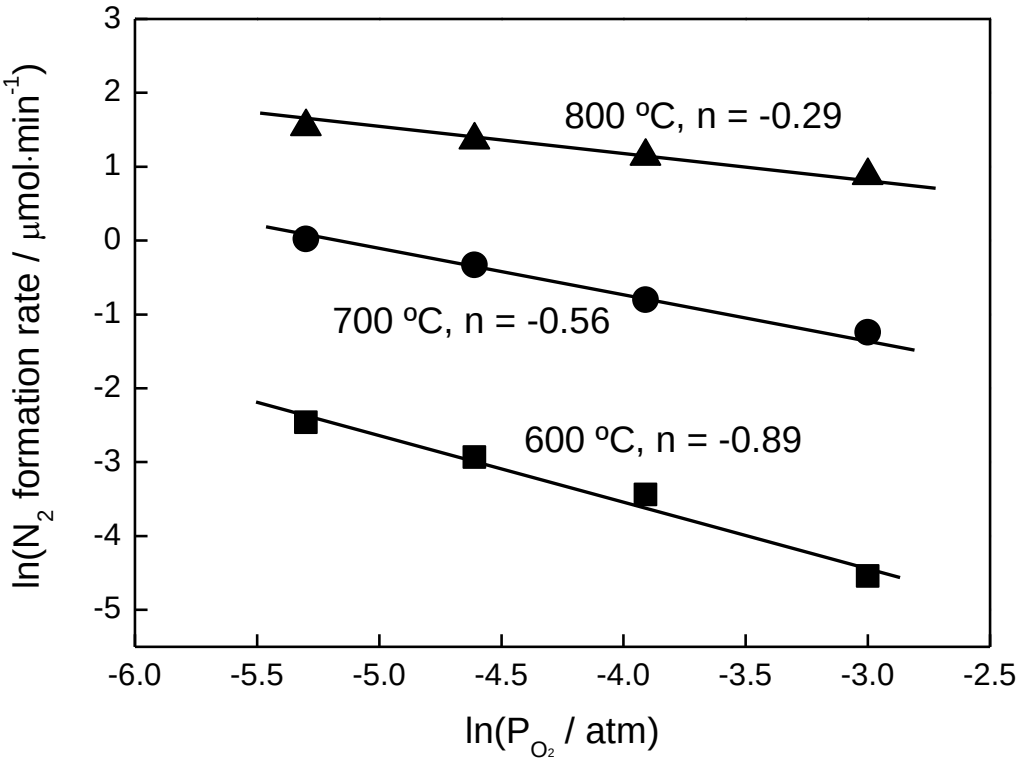

Figure 10. W.-J. Hong et al.